

On the Origin of Tilted Disks and Negative Superhumps

J. S m a k

N. Copernicus Astronomical Center, Polish Academy of Sciences,
Bartycka 18, 00-716 Warsaw, Poland
e-mail: jis@camk.edu.pl*Received*

ABSTRACT

The origin of tilted disks in cataclysmic variables is explained in terms of a model involving the stream-disk interactions. Tilted, precessing disk causes periodically variable asymmetry in the irradiation of the two hemispheres of the secondary component, resulting in variable vertical component of the velocity of the stream. The following stream-disk interactions provide additional vertical acceleration to disk elements needed to produce and maintain disk tilt. Predictions based on this model compare favorably with observations.

Key words: *accretion, accretion disks – binaries: cataclysmic variables, stars: dwarf novae*

1. Introduction

Negative superhumps are quite common among cataclysmic variables. They are present in dwarf novae of the SU UMa type during their superoutbursts and also among systems with stationary accretion – the permanent *negative* superhumpers (see Patterson 1999, Wood and Burke 2007, Olech et al. 2009 and references therein). Their periods are shorter than the orbital periods, the corresponding "period deficit" ε being correlated with the orbital period. There are examples of negative superhumpers showing also the *common* superhumps, the two types either being present simultaneously or switching from one type to another. In those cases the "period excess" of *common* superhumps and the "period deficit" of *negative* superhumps are correlated (cf. Olech et al. 2009).

The commonly accepted interpretation of negative superhumps explains them in terms of a tilted, precessing disk (cf. Patterson et al. 1993, Harvey et al. 1995, Patterson 1999, and references therein). Supporting this interpretation are: (1) the presence of light variations with P_{prec} observed commonly in such systems and (2) the fact that precession periods obtained from the observed values of P_{nsh} and P_{orb} agree reasonably well with theoretical predictions (see Larwood et al. 1996 and references therein).

Patterson et al. (1997) were the first to suggest that negative superhumps could be due to the "spot" produced by the variable stream impact as it transits across the surface of a tilted disk. More recently this was confirmed by Wood and Burke (2007) who used the 3D SPH simulations of a tilted, precessing disk to produce light curves closely resembling the observed superhumps (see also Montgomery 2009 and Wood et al. 2009).

The origin of the disk tilt, however, continues to be unknown. In particular, models proposed for other, more exotic objects (such as HZ Her or SS 433), are not applicable to the case of disks in cataclysmic variables (cf. Wood and Burke 2007 and references therein).

In the present paper we propose to explain the origin of tilted disks in cataclysmic variables in terms of a model involving the stream-disk interactions in a situation when the tilted, precessing disk causes variable irradiation of the two hemispheres of the secondary component and the resulting stream has periodically variable vertical velocity component.

We begin, in Section 2, with definitions and formulae to be used in further sections. Section 3 describes the irradiation controlled mass outflow and the next two sections are devoted to a detailed discussion of the resulting stream: its trajectory (Section 4) and its collision with the surface and edge of the disk (Section 5). The model, involving the stream-disk interactions, is presented in Section 6, its predictions being compared with observations in Section 7.

2. Definitions and Formulae

The precession period of a tilted disk is related to the orbital period and the negative superhump period by

$$\frac{1}{P_{prec}} = \frac{1}{P_{nsh}} - \frac{1}{P_{orb}}. \quad (1)$$

Accordingly we have

$$\phi_{prec} = \phi_{nsh} - \phi_{orb}, \quad (2)$$

with the zero-points of phases being defined as follows: $\phi_{orb} = 0$ at conjunction (in particular – at eclipse) and $\phi_{nsh} = 0$ at superhump maximum.

It will also be useful to recall that

$$\frac{d\phi_{nsh}}{d\phi_{orb}} = \frac{1}{1 - \varepsilon}, \quad (3)$$

where

$$\varepsilon = \frac{P_{orb} - P_{nsh}}{P_{orb}}, \quad (4)$$

is the negative superhump period deficit.

Let us now consider a disk with radius r_d , geometrical thickness z/r , and tilt angle δ . Its geometry (see Fig.1) is described by the following set of equations:

$$z_d = -z_o \cos \theta, \quad (5)$$

where θ is the position angle on the surface of the disk and

$$z_o = r_d \sin \delta, \quad (6)$$

and

$$z_t = z_d + \Delta z_d, \quad z_b = z_d - \Delta z_d, \quad (7)$$

$$\Delta z_d = r_d (z/r). \quad (8)$$

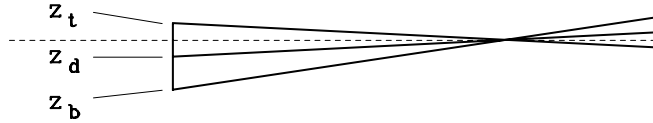


Fig. 1. Geometry of the tilted disk with $\delta = 3^\circ$ (see Section 7.1) and $z/r = 0.10$ at $\theta = 0$. Dotted line marks the orbital plane.

Two comments are worth adding here. First, that the specific value of the disk radius r_d is actually irrelevant since in what follows we will be dealing only with *angles*. Secondly, that all angles will be expressed here in units of phase, so that $\theta = 1$ corresponds to 2π or 360° .

Let us now consider an element of the outer disk. Its motion in the z -coordinate is described by Eq.(5) with

$$\theta = \frac{2\pi}{P_d} t, \quad (9)$$

where P_d is the period of oscillations (equal also to the period of revolution).

The acceleration, calculated from Eqs.(5) and (9), is

$$\frac{d^2 z}{dt^2} = z_o \left(\frac{2\pi}{P_d} \right)^2 \cos \theta + 2 \frac{dz_o}{dt} \left(\frac{2\pi}{P_d} \right) \sin \theta. \quad (10)$$

The second term on the right hand side of this equation implies that to produce and maintain disk tilt we need a mechanism capable of providing additional acceleration of the form

$$a_z \sim \sin \theta. \quad (11)$$

3. The Irradiation Controlled Mass Outflow

It has recently been shown (Smak 2008) that superoutbursts of Z Cha (and most likely of other dwarf novae) are due to a major enhancement in the mass outflow rate. This provides a strong argument in favor of the concept of irradiation controlled mass outflow. The details of this mechanism, however, still remain controversial (see Smak 2009b). The problem here is connected with the fact that the equatorial parts of the secondary, including L_1 , are in the shadow cast by the disk. The crucial question then is whether the material from irradiated regions flowing towards L_1 is still hot enough after reaching this point to produce substantial modulation of the mass outflow rate. Assuming that this is indeed the case it was possible to propose a new interpretation for superhumps (Smak 2009b). The simplicity and self-consistency of this interpretation could, in fact, be treated as an indirect argument in favor of this assumption.

In what follows we also assume that the outflow from L_1 is controlled by irradiation and, in particular, that in the case of variable irradiation there is a time delay between irradiation and the resulting dissipation at the point of impact (see Smak 2009b):

$$\Delta t = \Delta t_{flow} + \Delta t_{str} , \quad (12)$$

where Δt_{flow} is the time needed for the flow from irradiated regions to reach L_1 , and Δt_{str} is the time needed for the stream to reach the point of impact. The flow time Δt_{flow} depends, in general, on several parameters; in particular it depends on the distance between L_1 and the shadow boundary.

4. Stream Trajectories

When the disk is coplanar with the orbital plane the initial velocity vector of the stream at L_1 is of the form $\vec{v}_o = [v_{x,o}, v_{y,o}, 0]$. Let us, however, consider the case of a tilted disk when its part facing the secondary is tilted below the orbital plane (in the notation used in Section 6 this corresponds to $\theta_{2,d} = 0$). Compared to the coplanar case, the shadow boundary on the top hemisphere of the secondary is now closer to L_1 , while that on the bottom hemisphere – further away from L_1 . As a result, the contribution to the mass outflow from the material flowing from the top hemisphere is dominant and, consequently, the initial velocity vector now has a non-zero vertical component: $v_{z,o} < 0$.

To study the consequences of such a situation we calculate stream trajectories in three dimensions. For the initial stream velocity at L_1 we adopt various combinations of its components (in dimensionless units): $v_{x,o} = 0.01 - 0.05$, $v_{y,o} = (-0.01) - (-0.05)$, and $v_{z,o} = (-0.02) - (-0.05)$. Shown in Fig.2 are results obtained for the mass ratio $q = 0.3$ which corresponds to the typical periods

of negative superhumpers, as for example those listed below in Table 1. (Results obtained with other mass ratios were qualitatively the same).

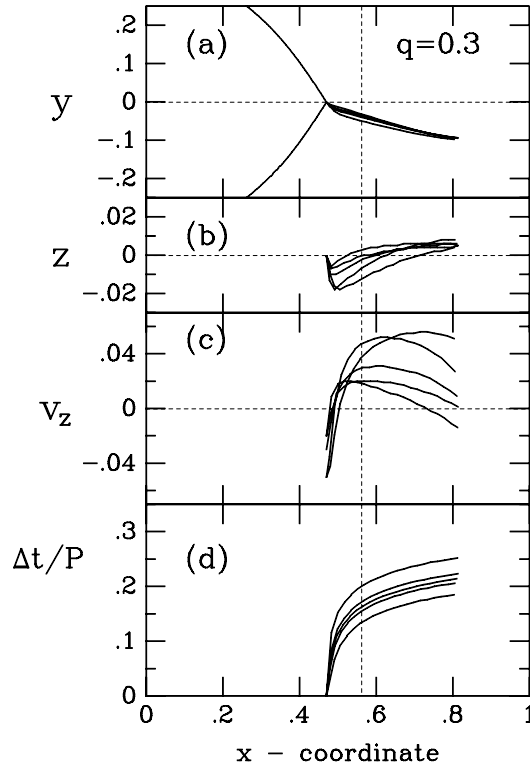


Fig. 2. (a) Stream trajectories in projection on the x-y plane. (b) Stream trajectories in projection on the x-z plane. (c) Vertical velocity component of the stream. (d) The "flight" time Δt_{str} in units of the orbital period. Vertical dotted line in all plots marks the location of the disk edge.

There are three important conclusions to be drawn from Fig.2: (1) The stream remains very close to the orbital plane. (2) The "flight" time from L_1 to $r = r_d$ is $\Delta t_{str} \approx 0.15P_{orb}$ and depends only weakly on the initial conditions. (3) At the point of impact the sign of the vertical velocity component of the stream is *opposite* to that of the initial velocity.

5. The Stream Overflow

The stream overflow was originally expected (cf. Smak 1985, Hessman 1999) to occur when the disk is geometrically thin, i.e. mainly in quiescent dwarf novae. Evidence is now available, however, for a substantial stream overflow in Z Cha during its superoutbursts (Smak 2007, 2009a). Besides, there is also theoretical evidence (Kunze et al. 2001) suggesting that this is indeed a much more common phenomenon.

Using disk geometry described in Section 2 we can calculate the fraction f_t of the stream material overflowing the top part of the disk and the fraction f_e colliding with disk edge. We adopt: $z/r = 0.10$ (cf. Smak 1992), $\delta = 3^\circ$ (see Section 7.1) and the density distribution in the stream given by the two-dimensional Gaussian formula with $\sigma/\Delta z_d = 0.5, 1.0,$ and 2.0 . With these assumptions we have

$$f_{t,e} = \int_{z_1}^{z_2} \frac{1}{2\pi\sigma} \exp(-z^2/2\sigma^2) dz, \quad (13)$$

where the integration limits are: $z_1 = z_t$ and $z_2 = \infty$ for f_t , and $z_1 = z_b$ and $z_2 = z_t$ for f_e .

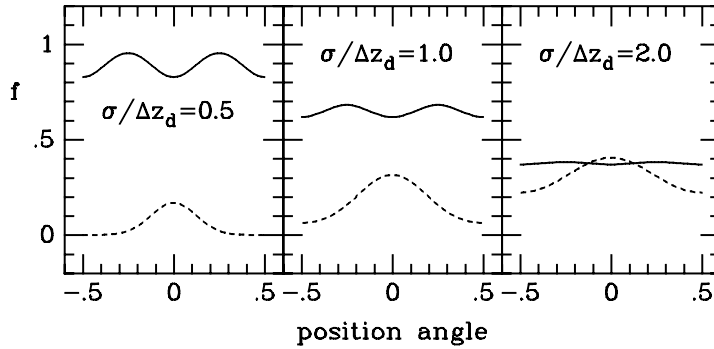


Fig. 3. The fraction f_t of the stream material overflowing the top part of the disk (broken lines) and the fraction f_e colliding with its edge (solid lines) are shown as a function of the position angle for $\delta = 3^\circ$ and for three values of σ .

Results are presented in Fig.3. As could be expected, substantial overflow occurs when σ is comparable to Δz_d . In particular, f_t becomes larger than f_e for $\sigma > 2\Delta z_d$. Furthermore, variations of f_t show only one maximum (and one minimum) per cycle, while those of f_e – two maxima (and two minima) per cycle (we shall return to this in Section 7.2).

Additional calculations were also made to reproduce the simple situation considered by Wood and Burke (2007) with the stream fully overflowing one side of the disk ($f_t \approx 1$). We find that this would require either much larger values of σ (which is rather unlikely) or tilt angles much larger than $\delta \sim 6^\circ$ (in fact, Wood and Burke used $\delta = 5^\circ$, but their disk was much thinner). We shall return to such a situation in Section 7.1.

6. The Model

The stream, colliding with the disk with non-zero vertical velocity component, is an obvious source of extra acceleration of disk elements. We propose that, under

suitable conditions, this can be the mechanism capable of producing and maintaining disk tilt.

The geometry of irradiation depends on the relative orientation of the tilted disk with respect to the secondary component. The position angle of the secondary with respect to the observer is

$$\theta_{2,obs} = \phi_{orb}^* . \quad (14)$$

The asterisk * is used here (and below) to emphasize that the phase refers to the moment of irradiation of the secondary component. The position angle of the lowest point of the disk, corresponding to $\theta = 0$ (as defined above), with respect to the observer is

$$\theta_{d,obs} = \phi_{prec}^* - \theta_o , \quad (15)$$

where θ_o is the precession phase at which the point with $\theta = 0$ is facing the observer. Note that $\theta_{d,obs}$, which changes due to retrograde precession, is counted in the direction opposite to $\theta_{2,obs}$. With this definition, the position angle of the disk point with $\theta = 0$ with respect to secondary component is

$$\theta_{d,2} = \theta_{d,obs} + \theta_{2,obs} = (\phi_{prec}^* + \phi_{orb}^*) - \theta_o = \phi_{nsh}^* - \theta_o . \quad (16)$$

Consequently, the vertical component of the terminal stream velocity at the point of impact v_{imp} can be expressed as a function of ϕ_{nsh}^* . Assuming, for simplicity, that its variations are cosinusoidal we can write

$$v_{imp} = v_{imp,o} \cos (\phi_{nsh}^* - \theta_o) , \quad (17)$$

where $v_{imp,o} > 0$ and corresponds to $\phi_{nsh}^* = \theta_o$ (see Fig.2c and Eq.16). The additional acceleration produced by the stream is then

$$a_{z,str} = \dot{M} v_{imp,o} \cos (\phi_{nsh}^* - \theta_o) \sim \sin [(\phi_{nsh}^* - \theta_o) + 0.25] . \quad (18)$$

The moment of impact is delayed with respect to the moment of irradiation by Δt (see Eq.12), the corresponding phase delays being $\Delta\phi_{orb} = \Delta t / P_{orb}$ (see Fig.2d) and $\Delta\phi_{nsh} = \Delta\phi_{orb} / (1 - \epsilon)$ (see Eq.3). The phase of impact is then

$$\phi_{nsh} = \phi_{nsh}^* + \Delta\phi_{nsh} = \phi_{nsh}^* + \frac{\Delta\phi_{orb}}{1 - \epsilon} , \quad (19)$$

and the position angle on the disk at the point of impact

$$\theta = \phi_{nsh}^* - \theta_o + \Delta\phi_{nsh} + \alpha = \phi_{nsh}^* - \theta_o + \frac{\Delta\phi_{orb}}{1 - \epsilon} + \alpha , \quad (20)$$

where α is the position angle of the impact point with respect to the line joining the two components. For $q = 0.3$ and at $r = r_d$ we have $\alpha \approx 0.014$ (in phase units).

The acceleration needed to produce and maintain disk tilt (Eq.11 in Section 2) must then be

$$a_z \sim \sin \left[(\phi_{nsh}^* - \theta_o) + \frac{\Delta\phi_{orb}}{1-\varepsilon} + \alpha \right]. \quad (21)$$

Comparing Eqs.(18) and (21) we immediately conclude that our proposed mechanism is most efficient when

$$\frac{\Delta\phi_{orb}}{1-\varepsilon} + \alpha = 0.25, \quad (22)$$

or, using $\varepsilon \approx 0.02$ and $\alpha \approx 0.014$, when

$$\Delta\phi_{orb} \approx 0.23. \quad (23)$$

In general the efficiency of this mechanism is described by the sign and value of the integral

$$\begin{aligned} W &= \int_0^1 \cos(\phi_{nsh}^* - \theta_o) \sin \left[(\phi_{nsh}^* - \theta_o) + \frac{\Delta\phi_{orb}}{1-\varepsilon} + \alpha \right] d(\phi_{nsh}^* - \theta_o) = \\ &= \pi \sin \left(\frac{\Delta\phi_{orb}}{1-\varepsilon} + \alpha \right), \end{aligned} \quad (24)$$

which implies that the mechanism is effective ($W > 0$) for

$$-0.02 < \Delta\phi_{orb} < 0.48. \quad (25)$$

The value of $\Delta\phi_{orb}$, estimated earlier (Smak 2009b) for three systems (IY UMa, DV UMa and OY Car) showing *common* superhumps, was found to be $\Delta\phi_{orb} = \Delta t/P_{orb} \approx 0.66$ which is clearly outside the range required by Eq.(25). This is not surprising, however, since those three objects do *not* show negative superhumps.

In the case of *negative* superhumpers with tilted disks the shadow boundary on the top (or bottom) hemisphere of the secondary is much closer to L_1 and this makes the flow time (Eq.12) much shorter. Consequently the value of $\Delta\phi_{orb}$ can easily be small enough to fulfill condition imposed by Eq.(25). To illustrate this point let us consider the extreme case, when the shadow boundary is close to L_1 (see Section 7.1). In such a case $\Delta t_{flow} \rightarrow 0$ and $\Delta\phi_{orb}$ becomes as small as $\Delta t_{str}/P_{orb} \approx 0.15$ (see Eq.12 and Fig.2d).

7. Model Predictions

7.1. Disk Tilts

Let us consider the situation when the tilt is so large that the vicinity of L_1 is fully exposed to direct irradiation. In such a case the vertical component of

the stream velocity becomes $v_{z,o} \equiv 0$ and the stream mechanism discussed in the previous Section no longer operates. This means that there is a natural upper limit to the tilt angle given by $\delta_{max} = \arcsin(z/r)$. Using values of $z/r = 0.10 - 0.12$ typical for hot disks we predict $\delta_{max} \approx 6 - 7^\circ$.

To test this prediction we analyze the best documented examples of negative superhumpers which show periodic light variations with P_{prec} . They are listed in Table 1, where the second and third columns contain the semi-amplitudes A of those variations and the orbital inclinations; in the case of non-eclipsing systems, with no estimates of inclinations being available, we adopt a range: $i = 20 - 60^\circ$.

Table 1
Semi-Amplitudes and Tilt Angles

Star	$A(\text{mag})$	$i(\text{deg})$	Refs.	$\delta(\text{deg})$
PX And	0.20	74	1,2	3
V603 Aql	0.07	20	3	7
TT Ari	0.07	29	4,5,6,7	4
TV Col	0.20	70	8,9,10	3
V751 Cyg	0.05	20-60	11	5-1
V1084 Her	0.08	20-60	12	6-2
V442 Oph	0.10	67	12,13	2

References: 1. Stanishev et al. (2002, Fig.5), 2. Thorstensen et al. (1991), 3. Patterson et al. (1997, Table 1), 4. Semeniuk et al. (1987, Fig.9), 5. Kraicheva et al. (1997), 6. Kraicheva et al. (1999), 7. Wu et al. (2002), 8. Barrett et al. (1988, Fig.4), 9. Hellier (1993), 10. Retter et al. (2003, Table 4), 11. Patterson et al. (2001, Fig.3), 12. Patterson et al. (2002, Figs.8 and 10), 13. Ritter and Kolb (1998).

The semi-amplitude A (in magnitudes) can be written as

$$A = \frac{dM_V}{di} \delta, \quad (26)$$

where dM_V/di describes the dependence of the observed luminosity of the disk on its inclination (or – generally – on the viewing angle).

At inclinations $i \leq 75^\circ$ it is sufficient to use the flat disk approximation giving

$$L_d(i) = \langle L_d \rangle \frac{6}{3-u} (1 - u + u \cos i) \cos i, \quad (27)$$

where u is the limb darkening coefficient for which we adopt $u = 0.6$. Turning to magnitudes we get

$$\frac{dM_V}{di} = 0.01895 \frac{(1 - u + 2u \cos i) \sin i}{(1 - u + u \cos i) \cos i} [\text{mag/deg}]. \quad (28)$$

The resulting values of δ are listed in the last column of Table 1. As one can see they are smaller than δ_{max} predicted above, the typical tilt being $\delta \approx 3^\circ$.

7.2. The Superhump Light Curves

The negative superhumps are thought to be due – primarily – to the collision of the stream with the surface of the tilted, precessing disk. There are two other effects, however, which must be considered. First, that part of the stream collides with disk edge (see Section 5). Secondly, that the outflow rate \dot{M} is likely to vary with variable geometry of irradiation, i.e. with $\theta_{d,2}$, or with ϕ_{nsh}^* .

Therefore the shape of the light curve can be formally written as

$$\ell(\phi_{nsh}) \sim \dot{M}(\phi_{nsh}^*) [f_e(\phi_{nsh}) + x f_i(\phi_{nsh})], \quad (29)$$

where ϕ_{nsh}^* is the phase at the moment of irradiation, ϕ_{nsh} – the phase at the moment of impact, and "x" in front of f_i is intended to represent the higher value of the impact parameter ΔV^2 in the case of the overflowing parts of the stream.

Limiting our discussion to qualitative considerations we recall (see Fig.3 in Section 5) that variations of f_i show one maximum (and one minimum) per cycle while those of f_e – two maxima (and two minima) per cycle. Variations of \dot{M} are also expected to show two maxima (and two minima) per cycle. Taking this into account we conclude that (1) the contribution from overflowing parts of the stream f_i must be dominant (due obviously to $x > 1$; see above), and (2) the contributions from variations of f_e and \dot{M} make the shape of the light curve significantly different from a simple cosine wave.

The second prediction is confirmed (at least qualitatively) by the observed shapes of negative superhump light curves which in nearly all cases (Barett et al. 1988, Fig.4; Patterson 2001, Fig.3; Patterson et al. 1997, Fig.4; Patterson et al. 2002, Figs.8,10,15; Stanishev et al. 2002, Fig.3) are clearly non-cosinusoidal.

7.3. The Light Variations with P_{prec}

The negative superhump maximum, which occurs – by definition – at $\phi_{nsh} = 0$, is produced when the stream is overflowing the top part of the disk at the position angle $\theta = 0$. Using Eqs.(19) and (20) we get

$$\theta_o = \alpha. \quad (30)$$

As mentioned in the Introduction, the mean luminosity of the disk varies with P_{prec} . The maximum of those variations occurs when $\theta_{d,obs} = 0$. Combining Eqs.(15) and (30) we then predict that it should occur at

$$\phi_{prec} = \alpha \approx 0.014 . \quad (31)$$

This agrees nicely with observations (e.g. TT Ari – Semeniuk et al. 1987, TV Col – Hellier 1993 and PX And – Stanishev et al. 2002) which show that the maximum occurs at $\phi_{prec} \approx 0$.

8. Discussion

The model presented in this paper appears quite simple and self-consistent. Its predictions compare favorably with observations. There are several problems and questions, however, which should be answered prior to considering it as fully acceptable.

(1) What makes the originally coplanar disk to become tilted? The qualitative answer to this question may be quite simple: when some part of the outer disk – due to a random fluctuation – is deflected above or below the orbital plane, then the mechanism described above can begin to operate. What conditions, however, are necessary for producing the positive feed-back (especially for condition given by Eq.25 to be fulfilled)?

(2) What is the cause of transitions from a tilted disk (with negative superhumps) to a coplanar disk (with common superhumps) – and *vice-versa* – observed in many systems (e.g. in V603 Aql or TT Ari; see references to Table 1)?

(3) How can we explain the simultaneous presence of negative and common superhumps in some systems (e.g. in V603 Aql or V503 Cyg; see references to Table 1)? And why are such cases so rare?

REFERENCES

- Barrett, P., O'Donoghue, D., Warner, B. 1988, *MNRAS*, **233**, 759.
 Harvey, D., Skillman, D.R., Patterson, J., Ringwald, F.A. 1995, *PASP*, **107**, 551.
 Hellier, C. 1993, *MNRAS*, **264**, 132.
 Hessman, F.V. 1999, *ApJ*, **510**, 867.
 Kraicheva, Z., Stanishev, V., Iliev, L., Antov, A., Genkov, V. 1997, *A&AS*, **122**, 123.
 Kraicheva, Z., Stanishev, V., Genkov, V., Iliev, L. 1999, *A&A*, **351**, 607.
 Kunze, S., Speith, R., Hessman, F.V. 2001, *MNRAS*, **322**, 499.
 Larwood, J.D., Nelson, R.P., Papaloizou, J.C.B., Terquem, C. 1996, *MNRAS*, **282**, 597.
 Montgomery, M.M. 2009, *MNRAS*, **394**, 1897.
 Olech, A., Rutkowski, A., Schwarzenberg-Czerny, A. 2009, *MNRAS*, *in press*.
 Patterson, J. 1999, *Disk Instabilities in Close Binary Systems*, Eds. S.Mineshige and J.C.Wheeler (Tokyo: Universal Academy Press), 61.
 Patterson, J., Thomas, G., Skillman, D.R., Diaz, M. 1993, *ApJS*, **86**, 235.
 Patterson, J., Kemp, J., Saad, J., Skillman, D.R., Harvey, D., Fried, R., Thorstensen, J.R., Ashley, R. 1997, *PASP*, **109**, 468.
 Patterson, J., Thorstensen, J.R., Fried, R., Skillman, D.R., Cook, L.M., Jensen, L. 2001, *PASP*, **113**, 72.
 Patterson, J. et al. 2002, *PASP*, **114**, 1364.

- Retter, A., Hellier, C., Augusteijn, T., Naylor, T., Bedding, T.R., Bembrick, C., McCormick, J., Velthuis, F. 2003, *MNRAS*, **340**, 679.
- Ritter, H., Kolb, U. 1998, *A&AS*, **129**, 83.
- Semiuk, I., Schwarzenberg-Czerny, A., Duerbeck, H., Hoffmann, M., Smak, J., Stępień, K., Tremko, J. 1987, *Acta Astron.*, **37**, 197.
- Smak, J. 1985, *Acta Astron.*, **35**, 351.
- Smak, J. 1992, *Acta Astron.*, **42**, 323.
- Smak, J. 2007, *Acta Astron.*, **57**, 87.
- Smak, J. 2008, *Acta Astron.*, **58**, 55.
- Smak, J. 2009a, *Acta Astron.*, **59**, 109.
- Smak, J. 2009b, *Acta Astron.*, **59**, 121.
- Stanishev, V., Kraicheva, Z., Boffin, H.M.J., Genkov, V. 2002, *A&A*, **394**, 625.
- Thorstensen, J.R., Ringwald, F.A., Wade, R.A., Schmidt, G.D., Norsworthy, J.E. 1991, *AJ*, **102**, 272.
- Wood, M.A., Burke, C.J. 2007, *ApJ*, **661**, 1042.
- Wood, M.A., Thomas, D.M., Simpson, J.C. 2009, *MNRAS*, *in press*, arXiv:0906.2713.
- Wu, X., Li, Z., Ding, Y., Zhang, Z., Li, Z. 2002, *ApJ*, **569**, 418.